Development of Multiple Beam Optical Tweezers

Dongjin Lee*†, Thomas W. LeBrun†, Arvind Balijepalli†, Jason J. Gorman†,
Cedric Gagnon†, Daehie Hong*, Esther H. Chang§
***Department of Mechanical Engineering , Korea University**
† National Institute of Standards and Technology, Gaithersburg, MD, USA
§ Department of Oncology, Georgetown University, Washington, DC, USA

ABSTRACT

This paper presents the design of a multiple beam optical tweezers instrument used for manipulating micro/nano-sized components. The basic equations used in designing the optical tweezers are derived and the stable and time-sharing multiple beam optical tweezers are constructed with scanning mirrors. The laser beam passes through a series of optical components such as lenses, mirrors, and scanning mirrors, and overfills the entrance aperture of microscope objective, which gives a stable trap. By rotating the laser beam with the scanning mirror, the focal positions are translated in the specimen plane and multiple micro/nano-sized objects can be moved. The constructed optical tweezers is used to manipulate cells and liposomes simultaneously and to trap multiple nano-wires. The experiments prove that the developed optical tweezers can be a very versatile manipulation tool for studying gene therapy and nano device fabrication.

Key Words: optical tweezers, optical trap, multiple optical traps, micro/nano manipulation, nano fabrication, micro/nano particle, nano-wire

1. Introduction

As nano and bio technologies have been extensively studied in academic and industrial sectors, the manipulation of micro/nano sized objects has become more and more important. Recently, researchers have begun to use optical tweezers for these purposes due to its inherent advantages.

Optical tweezers can apply forces up to a few hundreds piconewton (pN) with sub-pN resolution on objects whose characteristic dimensions are the order of the laser wavelength. It can also generate displacement up to a few tens of micrometers with nanometer resolution. If the optical tweezers is calibrated by adequate methods, such as the drag or escape force method, the equi-partition method, and the power spectral method [1], it can also be used as a force transducer. Optical tweezers has significant potential to dynamically manipulate multiple micro/nano-sized particles, to build up dynamic patterns, and to construct 2D or 3D micro/nano structures. In the near future, it can be applicable to Microfluidics, Lab-on-a-chip, and optical actuation of MEMS.

Optical tweezers has been used to manipulate micro/nano-sized objects in many fields such as biology [2-5], chemistry, colloidal physics, and polymer science in the form of single beam gradient force traps since Ashkin developed one for the first time in 1986 [6]. Recently, multiple beam optical tweezers have been developed in order to manipulate multiple particles simultaneously [7-11]. Multiple beam optical tweezers usually use the method of dividing one beam coming out of a laser into many beams by time sharing the beam between different traps using scanning mirrors.

This paper describes a new design of optical path for the multiple beam optical tweezers, where two scanning mirrors are utilized to expand effective working area in the specimen plane. The trapping performance of the newly designed optical tweezers is demonstrated in experiments of manipulating cancer cells and liposomes as well as nano-wires.

2. Trapping theory

Trapping force generation near a laser focus is generally understood using two approaches, Mie and Rayleigh scattering according to whether the laser wavelength λ is smaller or greater than the characteristic length of a particle to be trapped.

The Mie model is based on ray optics, where the diameter of a particle is large compared to the wavelength (typically, $R > 10\lambda$). In this model light is treated as a ray which has momentum. If light hits the surface of a micro/nano-sized object, it experiences reflection and refraction due to changes in the refractive index at the surface. The momentum change of the ray due to redirection induces an opposite momentum change in object by conservation of momentum, and the object experiences the resulting force. The resulting force can be resolved into two components, the scattering force which is parallel to beam propagation and the gradient force which is perpendicular to beam propagation. The radiation pressure force due to a single ray is given by Roosen et al. [12] as follows

$$F = \frac{n_m P}{c} Q \tag{1}$$

where n_m is the refractive index of surrounding media, P incident power of a ray, c speed of light, and Q a dimensionless force factor, where Q =1 corresponds to the case where a ray is completely absorbed and imparts no torque, e.g. simple radiation pressure. For reflection Q can be up to 2, but generally Q is much less than 1.

If a bundle of rays hits an object, as in a focused laser beam, the resultant force can be summed as scattering and gradient components with respect to the beam axis, as shown in Fig. 1. If the laser beam is cylindrically symmetric and passes through the center of a sphere, then the radial components of the gradient trapping force cancel by symmetry, and the resulting force is axial and directed to a point near the beam focus (Fig. 1a) if the sphere has a higher index of refraction than the surrounding medium. This neglects polarization effects, but under suitable conditions the effect of plane-polarization can be eliminated by symmetry [12].

More intense rays exert proportionately greater force on trapped particles, so in transverse trapping an object is drawn to the center of the beam as depicted with the thicker line in Fig. 1b. Because the incoming laser beam has a Gaussian intensity profile, the rays passing through the center of objective have more power, which means these rays exert more forces on the particle.

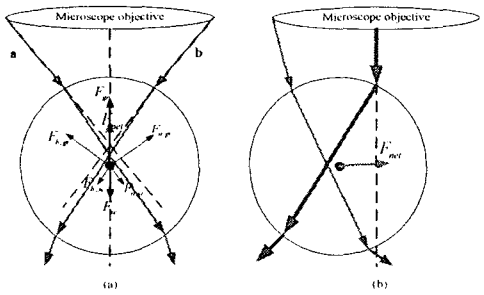

Fig. 1 Trapping of micro/nano sized particle in Mie regime: (a) Axial and (b) Transverse trapping

For cases when the particle is in an arbitrary position, the two trapping models above, axial and transverse trapping, can be superposed to explain the trapping mechanism.

If the characteristic length of the particle is small compared to wavelength of light, typically $R < 10\lambda$, the incident beam is treated as an electromagnetic wave. Fortunately, the interaction force of the particle with the electric field can be approximated as an electrostatic force [13]. The electromagnetic field induces an oscillating dipole, dipole moment, and induced electric field in the dielectric object. Accordingly, a new electric field $\mathbf{E}$ is formed by superposition of the original electric field and the induced electric field. Following Bechhoefer and Wilson [14], the energy of the particle due to new electric field is

$$W = UV = -\frac{1}{2}\mathbf{P}\cdot\mathbf{E}V = -\frac{1}{2}\alpha\varepsilon_m E^2 V \tag{2}$$

where U is the local energy density which is related to the dipole moment $\mathbf{P}$ and electric field $\mathbf{E}$. V represents the volume of the particle, ε_m the dielectric constant of the surrounding media, and E the magnitude of electric field. α represents the relative dielectric constants, as expressed by

$$\alpha = \frac{\varepsilon_p}{\varepsilon_m} - 1 \approx \frac{n_p^2}{n_m^2} - 1 \tag{3}$$

where n is index of refraction, and subscript p and m represent particle and surrounding media, respectively Spatial variation of the light intensity causes an energy change of the particle. The particle in the slowly spatially varying electric field (such as the focus forming of the microscope objective) experiences a force directed toward the point of (almost) highest intensity and minimum energy near the focus, since potential is proportional to $-I$. The magnitude of force is proportional to ∇I . The trapping force in the Rayleigh model is represented by

$$F_{sc} = n_m \frac{\langle S \rangle \sigma}{c} \tag{4}$$

$$F_{gr} = \frac{\varphi}{2} \nabla \langle E^2 \rangle \tag{5}$$

where n_m is refractive index of surrounding media, $\langle S \rangle$ is the time averaged pointing vector, σ is the scattering cross section in the surrounding medium, and φ is the polarizability of the particle [3].

3. Optical tweezers design

The basic instrument design is shown in Fig. 2. The telescope has two important functions, beam steering and magnification of beam size. The objective of the beam magnification is to fill the entrance aperture of the microscope objective, a key requirement to maximize trapping force for optical tweezers. The laser beam coming out of the laser head is not big enough to fill the objective entrance aperture and it is collimated and magnified to fill the entrance using the telescope. In addition, the telescope enables the laser beam to rotate about the entrance aperture by forming a conjugate plane to the plane of the entrance aperture at the scanning mirror using a pair of lenses. As a result when the scanning mirror rotates, the laser beam stays within the entrance aperture while it rotates, and the focal spot translates on the specimen plane in the X and Y directions.

Therefore, if the position of microscope objective is given, the position of scanning mirror can be determined by the following two constraints. First, the laser beam steered by the scanning mirror should rotate about the back aperture of the microscope objective (the mirror and objective aperture are in conjugate planes). Second, the laser beam at the objective entrance should be collimated since we are using an infinity corrected objective.

For a divergent laser beam, the basic optical tweezers setup and related parameters are shown in Fig. 2. Applying the first constraint yields,

$$d_{s1} = f_1 \frac{f_2 d_{12} - d_{2o}(d_{12} - f_2)}{f_2(d_{12} - f_1) - d_{2o}(d_{12} - f_1 - f_2)} \tag{6}$$

after solving successive lens equations. The distance of the two telescope lens is the sum of their focal lengths plus the added distance to collimate the divergent beam. That is,

$$d_{12} = f_1 + f_2 + \Delta d_{12} \tag{7}$$

Denote the distance between the laser and the first lens of the telescope as d_{l1}. Then, Eqn. (7) becomes

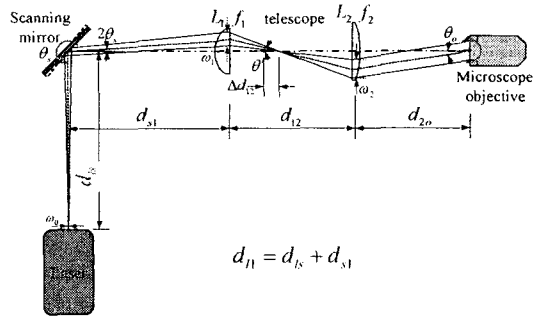

Fig. 2 Basic optical tweezers setup and related parameters

$$d_{12} = f_1 + f_2 + \frac{f_1'}{d_{l1} - f_1} \tag{8}$$

Consequently, the basic optical tweezers setup can be designed using equations (6) and (8) to satisfy both constraints. Given the desired diameter of the collimated output beam ω_2, the distance between the laser and the telescope d_{l1}, and the telescope length d_{12} can then be found by setting the telescope magnification.

If ω_1 is the beam width at the 1st lens of the telescope, rewriting the lens equation with respect to the beam diameters at the telescope lenses gives

$$\frac{f_1 + \frac{f_1^2}{d_{l1} - f_1}}{f_2} = \frac{\omega_1}{\omega_2} \tag{9}$$

Denoting the half-angle of the beam divergence out of the laser as D, the beam diameter at the first lens is expressed as

$$\omega_1 = \omega_0 + 2Dd_{l1} \tag{10}$$

Eliminating ω_1 from Equations (9) and (10), a 2nd order polynomial equation is obtained with respect to the distance between the laser and the telescope, that is,

$$Ad_{l1}^2 + Bd_{l1} + C = 0 \tag{11}$$

where

$$\begin{aligned} A &= 2f_2 D \\ B &= f_2\omega_0 - 2Df_1 f_2 - f_1\omega_2 \\ C &= -f_1 f_2 \omega_0 \end{aligned} \tag{12}$$

The scan range on the specimen plane can be calculated, assuming that the steering angle of the scanning mirror is very small (typically $\sim 4mrad$ for our piezo-mirrors). Simple geometric calculations yield the relationship between the angle of the scanning mirror θ_s, and the beam angle θ_o at the objective entrance aperture as,

$$\theta_o = -2\frac{f_1}{f_2}\theta_s \tag{13}$$

Using the concept of the effective focal length of the microscope objective lens, the transverse motion r in the specimen plane is related to the beam angle θ_o at the entrance aperture through

$$r = f_{EFL}\theta_o \tag{14}$$

Combining equations (13) and (14), one can see that a trapped sample can be manipulated up to the range of

$$r = -2f_{EFL}\frac{f_1}{f_2}\theta_s \tag{15}$$

To maximize the manipulating range, the ratio of the focal lengths of the telescope lens must be as large as practical. This means that the single telescope case, magnification should be maintained as small as possible.

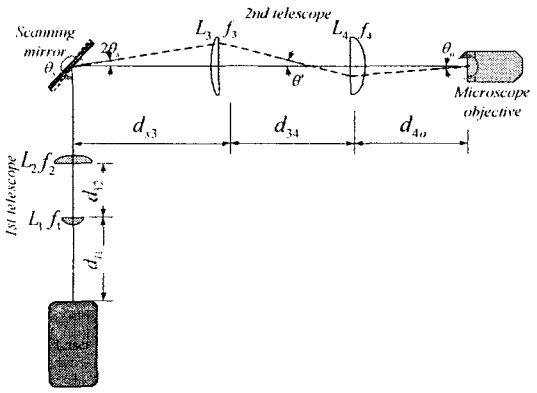

Fig. 3 Optical tweezers with two stage telescopes and related parameters

The single telescope optical tweezers shown in Fig. 2 only allows manipulation over a small range of a few micrometers for mirrors with a scan range of 2 mrad since the laser beam diameter is much smaller than the entrance aperture of the objective. However, the scanning area can be expanded by the insertion of one more telescope as shown in Fig. 3. In this case the beam size at the scanning mirror can be bigger than the objective entrance aperture, which means the magnification of the second telescope should be less than 1.

4. Experiments and results

4.1 Construction of dynamic optical tweezers

Fig. 4 shows the designed optical tweezers system built on a vibration isolation table (Newport) and Table 1 includes the design parameters for this system. The optical tweezers employs an inverted microscope (NIKON TE2000-E), an Nd:YVO4 laser (Spectra-physics, BL106-

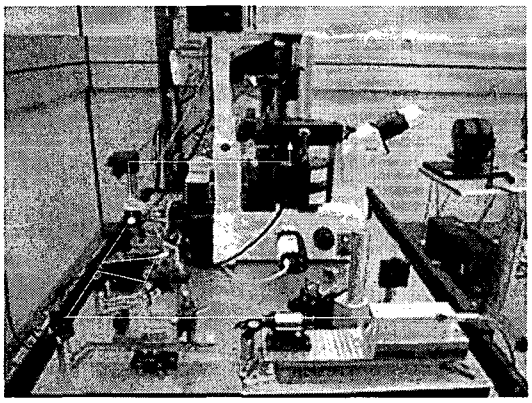

Fig. 4 Photograph of dynamic optical tweezers with two stage telescopes

Table 1 Design parameters of dynamic optical tweezers

Design Parameters	Nomenclature	Designed value
Distance	d_{f1}	376.4 mm
	d_{12}	111.3 mm
	d_{s3}	500 mm
	d_{34}	700 mm
	d_{4o}	200 mm(fixed)
Lens	f_1	11 mm
	f_2	100 mm
	f_3	500 mm
	f_4	200 mm
Laser beam	ω_0	0.42 mm
	ω_1	1.7 mm
	$\omega_2 = \omega_3$	15 mm
	ω_4	6 mm
	D	0.0017 rad

C, 1064nm), plano-convex lenses (Thorlabs), and an aspheric lens (Newfocus). The trapping laser passes through an isolator (Optics for Research, I0-2-YAG-VHP) for protecting laser head from reflected beam, a first telescope for beam expanding, two scanning mirrors (PI, S330) for increased scan range, and a second telescope for beam steering and beam expansion. The laser passes into the microscope and is bounced up into the microscope objective (Nikon, Plan Apo 60X/1.40 NA oil immersion) by a dichroic mirror (Chroma) that also allows imaging light to reach a CCD camera (Q IMAGING RETIGA Exi 1394). A motorized stage (PRIOR Scientific, Optiscan IS102) is used to position the sample in the microscope. The control program uses a NI digital-to-analog board (DAQ PCI 6052E) to generate a waveform that drives the piezo-mirror controller box (PI, E500) in the range of 0V to 10V. The control program integrates simulated traps and real video images from the CCD camera to represent the

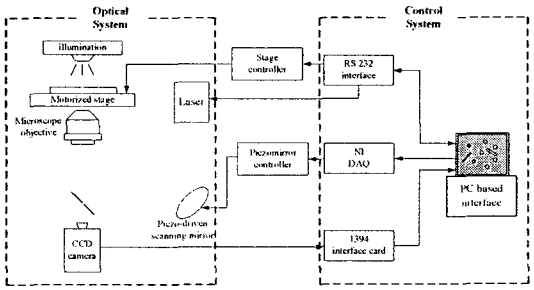

Fig. 5 Hardware block diagram of dynamic optical tweezers system

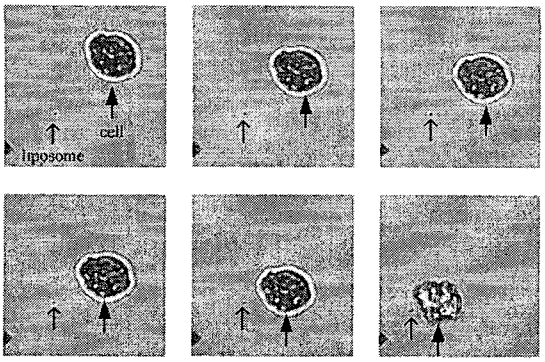

Fig. 6 Manipulation of cells and liposome using optical tweezers: the cell is approaching to the stationary liposome

workspace. Its functions include 멵reate traps? 멵ne trap? 멵elect/deselect traps? and 멵alibrate work area? etc. The overall hardware system is depicted in Fig. 5.

4.2 Sample manipulations

The constructed optical tweezers was used to manipulate human leukemia K562 cells and liposomes [17] for the future use in studies of their interactions for gene therapy. A liposome was maintained stationary, while the cell was manipulated toward the liposome. Fig. 6 depicts a series of pictures of manipulating processes. The small spot represents the liposome and the large one is the cancer cell. The cancer cell was dragged to the liposome and they were finally in contact each other in the last picture. The same cell was used in each image, but appeared different in the last image due to change of the focal plane.

The optical tweezers was also used to trap nano-wires

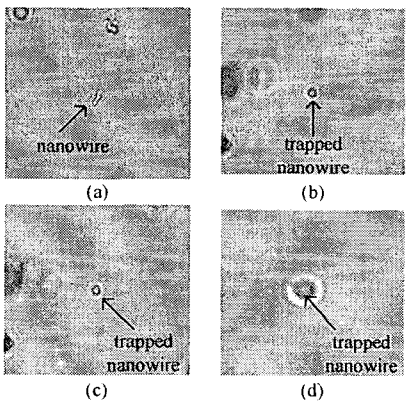

Fig. 7 Trapping nano-wire: (a) untrapped nanowire, (b) and (c) trapped nanowire, (d) enlarged picture of trapped nano-wire

as shown in Fig. 7. In Fig.7a, an untrapped nano-wire is shown, which has a long and curvy shape. Prior to trapping the nano-wire was floating in the medium experiencing high speed Brownian motion. When it was trapped, it was stationary and erected vertically because of trapping volume of laser (Fig. 7b and Fig. 7c). Fig. 7d represents an enlarged picture of trapped nano-wire.

5. Conclusion

This paper presented a new design of multiple beam optical tweezers that is dynamic, stable, and automated. A wide range of multiple traps was generated with dual stage telescopes and scanning mirrors. The tests of simultaneously manipulating cancer cells and liposomes, and nano-wires demonstrated the potential for a versatile tool for nano/bio device assembly and fabrication.

Acknowledgements

The authors would like to thank Kathleen Pirollo of Department of Oncology, Georgetown University, and Stephen Stranick and Babak Nikoobakht of NIST for providing the samples used here.

This work was supported by the Korea Research Foundation Grant (No. M07-2004-000-10280-0).

References

1. Singer, W., Bernet, S., Hecker, N., and RitschMarte, M., 빛hree-dimensional force calibration of optical tweezers,뀄J. Mod. Opt., Vol. 47, No. 14? 5, pp. 2921? 931, 2000
2. Sheetz, M.(ed), 밣aser tweezers in cell biology,? Methods in Cell Biology Series, Vol. 55, 1998.
3. Svoboda, K. and Block, S. M., 밼iological applications of optical forces,? Annu. Rev. Biophys. Biomol. Struct., Vol. 23, pp. 247? 85, 1994
4. Ashkin, A. and Dziedzic, J. M., 맕nternal cell manipulation using infrared laser traps,? PNAS, Vol. 86, pp. 7914? 918, 1989.
5. Ashkin, A. and Dziedzic, J. M., 밢ptical trapping and manipulation of single living cells using infrared-laser beams,? Ber. Bunsenges. Phys. Chem., Vol. 93, No. 3, pp. 254? 60, 1989.
6. Ashkin, A., Dziedzic, J. M., Bjorkholm, J. E., and Chu S., 밢bservation of a single-beam gradient force optical trap for dielectric particle,? Opt. Lett., Vol. 11, No. 5, pp. 288-291, 1986.

7. Visscher, K., Brakenhoff, G. J., and Krol, J. J., 밠icromanipulation by 멈ultiple? optical traps created by a single fast scanning trap integrated with the bilateral confocal scanning laser microscope,? Cytometry, Vol. 14, No. 2, pp. 105-114, 1993.
8. Visscher, K., Gross, S. P., and Block, S. M., 밇onstruction of multiple-beam optical traps with nanometer-resolution position sensing,? IEEE J. Sel. Top. Quantum Electron., Vol. 2, No. 4, pp. 1066-1076, 1996.
9. Fallman, E. and Axner, O., 밇esign for fully steerable dual-trap optical tweezers,? Appl. Opt., Vol 36, No. 10, pp. 2107-2113, 1997.
10. Mio, C., Gong, T., Terray, A., and Marr, D. W. M., 밇esign of scanning laser optical trap for multiparticle manipulation,? Rev. Sci. Intr., Vol. 71, No. 5, 2000.
11. Duffresne, E. R., Spalding, G. C., Dearing, M. T., Sheets, S. A., and Grier, D. G., 밇omputer-generated holographic optical arrays,? Rev. Sci. Instum., Vol. 72, No. 3, pp. 1810-1816, 2001.
12. Ashkin, A., 밠orces of a single-beam gradient laser trap on a dielectric sphere in the ray optics regime,? Biophys. J., Vol. 61, pp. 569-582, 1992.
13. Purcell E. M., 밇lectricity and magnetism,? Mcgraw-Hill book company, pp. 298-330, 2003.
14. Bechhoefer, J and Wilson, S., 밠aster, cheaper, safer optical tweezers for the undergraduate laboratory,? Am. J. Phys., Vol. 70, No. 4, pp. 247-85, 2002.
15. Tlusty, T., Meller, A., and Bar-Ziv, R., 밠ptical gradient forces of strongly localized fields,? Phys. Rev. Lett., Vol. 81, pp. 1738-1741, 1998.
16. Smith, S. P., Bhalotra, S. R., Brody, A. L., Brown, B. L., Boyda, E. K., and Prentiss, M., ? Inexpensive optical tweezers for undergraduate laboratories,? Am. J. Phys., Vol. 67, No. 1, pp. 26-35, 1999.
17. Xu, L., Frederik, P., Pirollo, K. F., Tang, W. H., Rait, A., Xiang, L. M., Huang, W., Cruz, I., Yin, Y., Chang, E. H., 밠elf-assembled virus-mimicking nanostructure for high efficiency tumor-targeted gene delivery,? Human Gene Therapy, Vol. 13, pp.469-481, 2002.